Aggregation and hemi-fusion of anionic vesicles induced by the antimicrobial peptide cryptdin-4

Jason E. Cummings, T. Kyle Vanderlick *

Department of Chemical Engineering, Princeton University, Princeton, NJ 08544, USA

Abstract

We show that cryptdin-4 (Crp4), an antimicrobial peptide found in mice, induces the aggregation and hemi-fusion of charged phospholipid vesicles constructed of the anionic lipid POPG and the zwitterionic lipid POPC. Hemi-fusion is confirmed with positive total lipid-mixing assay results, negative inner monolayer lipid-mixing assay results, and negative results from contents-mixing assays. Aggregation, as quantified by absorbance and dynamic light scattering, is self-limiting, creating finite-sized vesicle assemblies. The rate limiting step in the formation process is the mixing of juxtaposed membrane leaflets, which is regulated by bound peptide concentration as well as vesicle radius (with larger vesicles less prone to hemi-fusion). Bound peptide concentration is readily controlled by total peptide concentration and the fraction of anionic lipid in the vesicles. As little as 1% PEGylated lipid significantly reduces aggregate size by providing a steric barrier for membrane apposition. Finally, as stable hemi-fusion is a rare occurrence, we compare properties of Crp4 to those of many peptides known to induce complete fusion and lend insight into conditions necessary for this unusual type of membrane merger.
© 2007 Elsevier B.V. All rights reserved.

Keywords: Peptide; Aggregation; Hemi-fusion; Cryptdin-4; Defensin; Vesicles

Aggregation and juxtaposition of lipid membranes is an essential step in the ubiquitous process of membrane fusion within biological systems. Events such as endo- and exocytosis, fertilization, and even cellular infection by viruses, all require the apposition of two or more lipid-enveloped entities. Similarly, aggregation is also important within model membrane systems such as vesicle or liposome suspensions. Here, it is often an unwanted event, complicating fundamental studies designed to probe the interactions of various membrane-active molecules with lipid membranes. On the other hand, vesicle aggregation can be a positive outcome, either as a precursor to desired fusion events or simply as a means to purposefully segregate or condense soluble membrane material.

Upon aggregation, vesicles may simply remain as individual entities or they can unite and share lipids. When intermembrane lipid-mixing occurs, two outcomes are possible. One is hemi-fused vesicles, where only the lipids within the outer membrane leaflets of adjacent vesicles mix. The other is completely fused vesicles, where both leaflets of adjacent membranes experience lipid-mixing. Hemi-fusion maintains the interior aqueous regions of each vesicle as separate compartments, while complete fusion merges vesicle contents. Hemi-fusion is rarely a sustained state, more often existing only as an intermediate step on the path to complete fusion [1,2]. Though unusual, stable hemi-fused vesicles may prove particularly useful for various applications, such as multi-compartment drug delivery vehicles.

Aggregation is not usually a spontaneous process; it often requires an aggregate-inducing agent. The identity of this agent frequently determines if membrane and/or contents-mixing will occur within the aggregated structure. Polymers such as polyethylene glycol (PEG), multivalent ions like Ca^{+2}, and membrane-active peptides such as those found in viruses are some of the most well studied aggregate-inducing agents. Both PEG [3,4] and Ca^{+2} [5] have been found to cause complete fusion of phospholipid vesicles. Peptides on the other hand, exhibit a variety of behaviors. The α-helical peptide penetratin

---

* Corresponding author. Tel.: +1 609 258 4891; fax: +1 609 258 0211.
  E-mail address: vandertk@princeton.edu (T.K. Vanderlick).

aggregates vesicles without the occurrence of any type of fusion [6,7]. Other α-helical peptides, such as the influenza virus fusion peptide [8–10] or the HIV fusion peptide [11,12], induce complete fusion within biological and model membrane systems, while a mutant of the influenza virus fusion peptide has exhibited hemi-fusion inducing properties [13]. We note that although many α-helical peptides share the ability to facilitate aggregation/fusion among vesicle membranes, this trait is not specific to that secondary structure. Fujii et al. have reported that several β-sheet peptides found in humans and rabbits induce the complete fusion of anionic membranes [14]. Also, myelin basic protein, which can possess both a-helical and b-sheet portions, induces the hemi-fusion of phospholipid vesicles [15].

Peptides bearing α-helical structure have been the subject of numerous fusion studies [8,9,11,16–20], while the fusogenic properties of peptides assuming a β-sheet structure are still largely unexplored. Membrane interactions of β-sheet peptides and α-helical peptides are not expected to be similar, with differing conformational changes, angles/depths of insertion, oligomerization properties, etc. Hence, exploring the fusogenic abilities of β-sheet peptides, and comparing them with those of α-helical peptides, could lead to information regarding prerequisites for the occurrence of fusion.

Of particular importance within the family of β-sheet peptides is a class of peptides known as defensins. These peptides exist within the innate immune system of mammals, plants, and insects, and have been the subject of various membrane-interaction studies [21–27]. The most well studied defensins include those isolated from humans, rabbits, and mice. Several human and rabbit defensins, as mentioned earlier, have been reported to cause complete fusion within a system of anionic vesicles [14]. The fusogenic properties of mouse defensins, however, have never been explored.

In this paper, we examine the ability of the mouse defensin cryptdin-4 (Crp4) to induce vesicle aggregation and membrane fusion. This peptide is one of several cryptdins secreted by the mouse small bowel and was found to be the most potent in bactericidal assays conducted with Crp1–Crp6 [28]. Crp4 (sequence: GLLCYCRKGHCKRGERVRGTCGIRFLYCCPRR) assumes a β-sheet structure stabilized by three disulfide bonds. It has a molecular mass of about 3.8 kDa and possesses a large net charge of +8.5 at physiological pH, a characteristic arising from its high content of arginine residues. Here we show that Crp4 is capable of inducing hemi-fused vesicle aggregates. The aggregation/hemi-fusion process can be controlled by altering vesicle size as well as membrane composition. We also show how the incorporation of lipid-anchored polyethylene glycol into the vesicle membrane inhibits the aggregation/hemi-fusion process.

1. Materials and methods

1.1. Peptide

Cryptdin-4 was purchased from New England Peptide, Inc. (Gardner, MA). The peptide was synthesized by solid phase peptide synthesis and was verified by HPLC and amino acid analysis. Crp4 was >95% pure. Explicit tests were not performed to determine if the folded structure of the peptide was correct. However, bactericidal assays and membrane leakage assays performed with this peptide and with Crp4 peptide from the research group of Andre Ouellette at the University of California-Irvine, Department of Pathology and Laboratory Medicine, showed identical results. The folded structure of the latter had been confirmed. Therefore, due to the consistency of the assays with the two sets of peptide, we assumed that the purchased peptide was also folded correctly.

1.2. Lipids

1-palmitoyl-2-oleoyl-sn-glycero-3-[phospho-rac-(1-glycerol)] (POPG), 1-palmitoyl-2-oleoyl-sn-glycero-3-phosphocholine (POPC), 1,2-dioleoyl-sn-glycero-3-phosphoethanolamine-N-(7-nitro-2-1,3-benzoxadiazol-4-yl) (NBD-DOPE), 1,2-dioleoyl-sn-glycero-3-phosphoethanolamine-N-(lissamine rhodamine B sulfonyl) (RH-DOPE), and 1,2-dipalmitoyl-sn-glycero-3-phosphoethanolamine-N-[methoxy(polyethylene glycol)-2000] (PEG2000-DPPE) were all purchased from Avanti Polar Lipids (Alabaster, AL).

1.3. Chemicals and reagents

8-aminonaphthalene-1,3,6-trisulfonic acid (ANTS), p-xylene-bis-pyridinium bromide (DPX), and 1,1′-dioctadecyl-3,3,3′,3′-tetramethylindodicarbo-cyanine-5,5′-disulfonic acid (DiIC$_{18}$(5)-DS) were purchased from Molecular Probes (Eugene, OR). Unless otherwise stated, all other chemicals were from Sigma-Aldrich (St. Louis, MO), of the highest grade available, and used as received. Water was produced by a Milli-Q UF unit (Millipore, Bedford, MA) and had a resistivity of 18.2 MΩ-cm.

1.4. Preparation of liposomes

Small unilamellar vesicles (SUVs) were prepared by sonication of multilamellar vesicle (MLV) dispersions for 1 h as performed with a VirTis VirSonic 100 titanium tip sonicator. The MLV dispersions were formed by hydrating dried lipid films (3 mL of buffer) and subjecting them to 5 cycles of vortex-freeze–thaw.

Large unilamellar vesicles (LUVs) were prepared not by sonication, but rather by extruding (Lipex Biomembranes Inc) the MLV dispersion twice through a 400-nm (diameter) polycarbonate filter (Nucleopore Co.), followed by 10 times through either a 100-nm (diameter) or 300-nm (diameter) polycarbonate filter, which generates vesicles of the nearly the same respective size as determined using dynamic light scattering (DLS).

Giant unilamellar vesicles (GUVs) were created using a modification of the electroformation method [29,30]. 50 μl of a 0.5-mg/ml lipid solution was spread on platinum electrodes that were held 5 mm apart in a Teflon/glass cell. Films were dried under vacuum overnight to remove trace solvent. An aqueous solution was added to the cell, and vesicles were formed by the application of a 1.0-V sine wave across the electrodes.

Lipid concentrations were determined using a phosphorus assay explained in a procedure made available by Avanti Polar Lipids (www.avantilipids.com).

1.5. Vesicle aggregation measurements

Kinetic absorbance measurements were employed to continuously monitor vesicle aggregation. These measurements were carried out on a Spectronic Genesys 2 UV-Vis spectrophotometer at 436 nm with a total sample volume of 2 ml. The lipid concentration of the sample was 50 μM while the peptide concentration was adjusted according to the range of peptide to lipid molar ratios studied. Dynamic light scattering experiments were performed using a commercial apparatus [Brookhaven, Inc., BI-200SM laser light scattering goniometer equipped with a solid-state laser (λ=532.5 nm) and an ALV-5000 correlator]. All measurements were performed at 25 °C under a scattering angle of 90°. The lipid concentration of DLS samples was 1 mM, with peptide concentrations adjusted so that the same peptide to lipid molar ratios were used as in absorbance measurements.

1.6. Total lipid-mixing assay

Lipid-mixing was determined by a fluorescence resonance energy transfer method using two lipid-anchored probes: NBD-DOPE and RH-DOPE [31]. In short, the assay tracks the average separation of these two probes as lipid is

redistributed through vesicle membrane mixing. Three sets of lipid chloroform solutions are prepared for the assay: (1) POPG/POPC solution (this assay was conducted at various ratios of the two lipids and exact ratios can be seen in Results and the captions of Figs. 3 and 6) containing 0.8 mol% of each of the fluorescently labeled lipids, (2) POPG/POPC solution of the same composition but without the fluorescent lipids, and (3) POPG/POPC solution containing 0.08 mol% of each fluorescent lipid (calibration lipid solution). Lipid solutions are dried under vacuum for 4 h and then, in the cases of SUVs and LUVs, hydrated with an aqueous solution of 130 mM NaCl and 10 mM HEPES (260 mOsm/L, pH 7.4). For creating GUVs, the dried lipid is hydrated with a 260-mM Glucose and 10 mM HEPES (260 mOsm/L, pH 7.4) solution but is later diluted in the solution used for creating SUVs and LUVs. Aliquots from the labeled and unlabeled vesicles are mixed at a 1:9 ratio to create a total lipid concentration of 50 μM in a 2-ml volume. The excitation wavelength is set at 460 nm while the emission wavelength is set at 530 nm. The minimal fluorescence originating from this solution is set as the 0% fluorescence. 100% fluorescence is determined from a 50-μM solution of the calibration vesicles. The fraction of lipid-mixing occurring as the result of the introduction of peptide to the labeled and unlabeled vesicle solution is calculated as

$$\text{Fraction of Lipid} - \text{Mixing} = \frac{F(t) - F_o}{F_\infty - F_o} \tag{1}$$

where $F(t)$ is the fluorescence intensity at time t, F_o is the minimal fluorescence, and F_∞ is the fluorescence of the calibration vesicles. The fluorescence originating from a solution of calibration vesicles (F_∞) remains constant even after addition of peptide. The limiting value for a system undergoing full fusion would be 1.0, and would be 0.5 if only hemi-fusion occurred (or somewhat greater if the amounts of lipid on the inner and outer bilayer leaflets were not equal).

1.7. Inner monolayer lipid-mixing assay

The general idea of this assay is to selectively label the inner monolayer of vesicles with FRET pairs. This is accomplished by formulating vesicles with probes throughout the membrane (i.e., on both monolayers) and then incapacitating those residing in the outer leaflet with the addition of a reducing agent [32]. As with the total lipid-mixing assay, monolayer mixing is revealed by an increase in fluorescence as the FRET pairs change their average separation. Three sets of lipid chloroform solutions are prepared for this assay: (1) POPG solution containing 0.8 mol% NBD-DOPE and 0.8 mol% DiIC$_{18}$(5)-DS, (2) POPG only solution, and (3) POPG solution containing 0.08 mol% NBD-DOPE and 0.08 mol% DiIC$_{18}$(5)-DS (calibration lipid solution). Lipid solutions are dried under vacuum for 4 h and LUVs (~100 nm diameter) are then created after hydrating the dried film with an aqueous solution of 130 mM NaCl and 10 mM HEPES (260 mOsm/L, pH 7.4). Inner monolayer labeled vesicles are created by adding sodium dithionite to preformed vesicles of (1) and (3). Sodium dithionite eliminates the fluorescence originating from the outer monolayer of the vesicles and reduces the sample fluorescence by approximately 50%. Excess sodium dithionite is removed from solution on a Sephadex G-50 column using a 130-mM NaCl and 10 mM HEPES (260 mOsm/L, pH 7.4) aqueous solution as the eluant. Aliquots from (1) and (2), where (1) has been exposed to sodium dithionite, are then mixed at a 1:9 ratio to create a total lipid concentration of 50 μM in a 2-ml volume. The excitation wavelength is set at 460 nm while the emission wavelength is set at 530 nm. The minimal fluorescence originating from this solution is set as 0% lipid-mixing. 100% lipid-mixing is associated with the fluorescence of a 50-μM solution of (3) after exposure to sodium dithionite. The fraction of lipid-mixing occurring as the result of the introduction of peptide to the solution of (1) and (2) is calculated as shown above for the total lipid mixing assay.

1.8. Contents-mixing assay

The mixing of the aqueous contents of vesicles was monitored with an assay utilizing the fluorophore-quencher system of ANTS-DPX [31]. In short, this assay tracks the decrease in fluorescence as ANTS-filled vesicles merge contents with DPX-filled vesicles. Three identical lipid compositions of POPG and POPC in chloroform are dried under vacuum for 4 h. Each of the lipid films is

then hydrated with one of the following solutions: (1) 25 mM ANTS, 90 mM NaCl, 10 mM HEPES (260 mOsm/L, pH 7.4), (2) 90 mM DPX, 50 mM NaCl, 10 mM HEPES (260 mOsm/L, pH 7.4), (3) a 1:1 mixture of solutions 1 and 2. LUVs are then created in the manner described above. Vesicles are separated from unencapsulated fluorophore and quencher on a Sephadex G-50 column using a 130-mM NaCl and 10 mM HEPES (260 mOsm/L, pH 7.4) aqueous solution as the eluant. Equal amounts of ANTS-loaded and DPX-loaded vesicles are mixed together to create a final lipid concentration of 50 μM in a 2-ml volume. The fluorescence originating from this solution is the maximum fluorescence, with the excitation wavelength of the spectrophotometer set at 360 nm while the emission wavelength is set at 530 nm. The fluorescence generated by a 50-μM solution of ANTS-DPX-loaded vesicles is the minimum fluorescence. Contents-mixing is calculated as

$$\text{Fraction of Contents} - \text{Mixing} = \frac{I_o - I(t)}{I_o - I_\infty} \tag{2}$$

where $I(t)$ is the fluorescence intensity at time t, I_o is the maximum fluorescence, and I_∞ is the minimum fluorescence.

2. Results

2.1. Turbidity

Turbidity, as described by absorbance, provides a numerical measure of the degree of aggregation. Fig. 1 shows such time dependent measurements as POPG LUVs (~100 nm diameter) are added to peptide at peptide to lipid molar ratios between 0 and 0.05. As can be seen, an increase in sample absorbance occurs immediately following lipid injection, with higher extents correlated with higher concentrations of Crp4. The rate of absorbance increase is initially fast but slows as aggregation continues. After an hour, the absorbance readings appear to have reached a stable value.

2.2. Dynamic light scattering

To further characterize the aggregation process, we employ dynamic light scattering (DLS) to determine aggregate sizes. POPG LUVs with radii of 47 nm, as measured using DLS, were
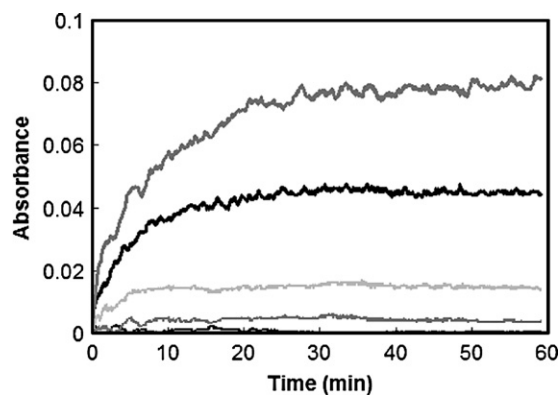

Fig. 1. Absorbance measurement of Crp4-induced vesicle aggregation. Samples of POPG LUVs (~100 nm diameter) at 50 μM were created and Crp4 was added to bring the peptide-to-lipid ratio in the samples to 0 (thin black line), 0.01 (thin dark gray line), 0.02 (thin light gray line), 0.035 (thick black line), and 0.05 (thick dark gray line). Absorbance of the samples increases immediately following the injection of Crp4 due to the creation of vesicle aggregates. Higher concentrations of Crp4 induce greater aggregation.
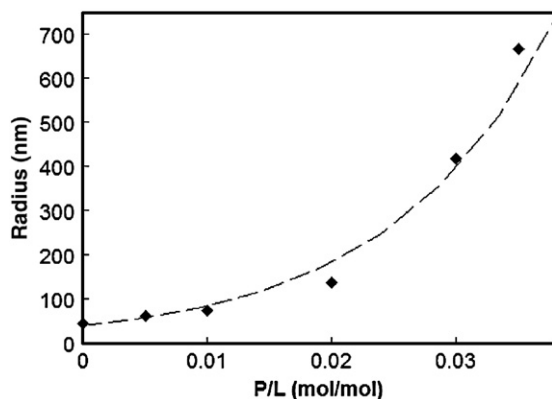
Fig. 2. DLS measurements of vesicle size. 1 mM solutions of POPG LUVs with radii of 47 nm were subjected to Crp4 and allowed to incubate for 1 h. Aggregate size increases with increasing peptide-to-lipid molar ratios until precipitates can be seen settling out of solution at $P/L > 0.035$. The dashed line demonstrates the Arrhenius nature describing the size increase of vesicle aggregates.

mixed with various amounts of Crp4 and allowed to incubate for 1 h, a time at which absorbance measurements suggest that aggregate growth has stopped. Fig. 2 plots the stable aggregate size as a function of peptide to lipid molar ratio. The dashed line demonstrates the exponential scaling of aggregate size with P/L. At P/L values greater than 0.035, precipitates can be seen forming and settling out of solution.

We note that DLS can produce erroneous data when extraneous forces, such as those leading to vesicle aggregation, disturb the natural Brownian motion of particles in solution. Our measurements were made after aggregation had stabilized and therefore should be indicative of the correct average hydrodynamic radius of the aggregates, to the extent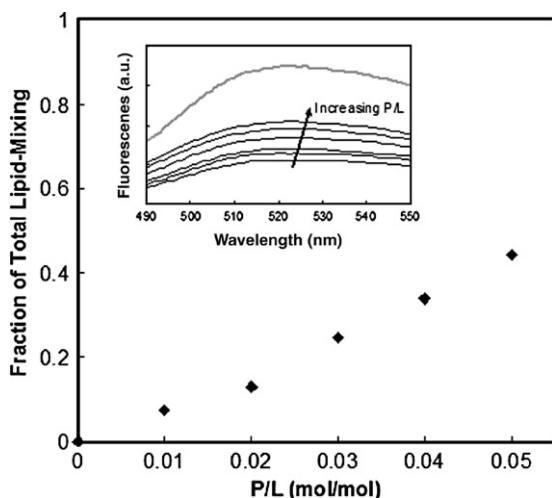 that they can be represented as spherical entities. At the very least, we get a qualitative trend representative of how aggregate size is increasing with P/L.

2.3. Lipid-mixing and contents-mixing assays

Total lipid-mixing was monitored by following changes in the amount of quenching between fluorescent lipid probes after addition of Crp4 (as a result of redistribution of lipids between vesicles (see Materials and methods)). The vesicle suspension consisted of a 1:9 mixture of 98.4 POPG/0.8 NBD-DOPE/0.8 RH-DOPE:POPG. In Fig. 3, the fraction of total lipid-mixing is plotted versus peptide to lipid molar ratio, revealing a direct dependence of lipid-mixing on peptide concentration. The fraction of total lipid-mixing reaches a value of ~0.45 at a $P/L = 0.05$. This result affirms the occurrence of some level of membrane fusion, whether it is hemi-fusion or complete fusion.

A second lipid-mixing assay, where the fluorescence from the vesicle membranes' outer monolayer is eliminated by the addition of an aqueous reducing agent, reveals the extent of lipid mixing between the inner monolayers of vesicles in solution. The vesicle system utilized for this assay consisted of a 1:9 mixture of 98.4 POPG/0.8 NBD-DOPE/0.8 DiIC$_{18}$(5)-DS:POPG. Shown in Fig. 4A is the emission spectrum for vesicles before the probes in the outer monolayer are incapacitated; Fig. 4B shows the reduction in fluorescence upon adding the reducing agent sodium dithionite. If peptide is added to these vesicles the spectra show no change (black lines in Fig. 4 corresponding to 5 different P/L values). As a point of reference we note that had inner monolayer mixing occurred in all vesicles, Fig. 4C would represent the
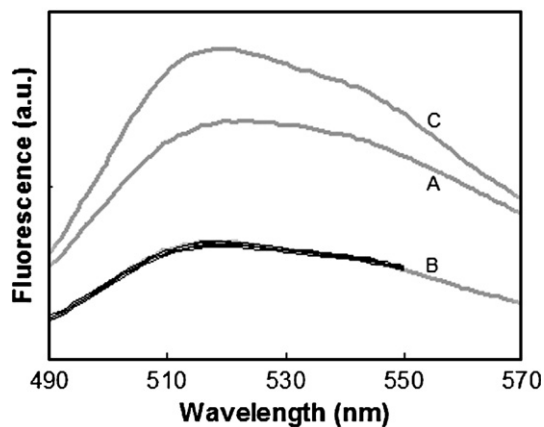

Fig. 3. Total lipid-mixing assay. Various concentrations of Crp4 were added to 50 μM solutions of POPG and 98.4 POPG/0.8 NBD-DOPE/0.8 RH-DOPE LUVs (~100 nm diameter). A change in the amount of quenching in the fluorescently labeled vesicles is an indication of lipid-mixing and is quantified as described in Materials and methods. Each black line in the inset is the fluorescence spectrum of a system of vesicles where peptide is present at P/L ratios of 0 to 0.05. The gray line is the fluorescence spectrum that would result if 100% lipid mixing occurred.

Fig. 4. Inner monolayer lipid-mixing assay. Various concentrations of Crp4 were added to 50 μM solutions of POPG and 98.4 POPG/0.8 NBD-POPE/0.8 DiIC$_{18}$(5)-DS LUVs (~100 nm diameter), where the fluorescence from the outer monolayer of the latter had been eliminated by the addition of sodium dithionite. Lipid-mixing is revealed by a change in the amount of quenching in the fluorescently labeled vesicles. Curve A is the fluorescence spectrum from a solution of vesicles where both monolayers of the labeled vesicles are fluorescing. Curve B is the fluorescence spectrum of a solution of vesicles where the fluorescence of the outer monolayer of the labeled vesicles has been incapacitated (~50% of curve A). The thin blank lines that coincide with curve B are the resulting spectra when peptide at P/L ratios between 0.01 and 0.05 are added to the vesicle solution represented by curve B. No change in quenching (i.e., no lipid-mixing) is evident with addition of Crp4. Curve C is the fluorescence spectrum that would result if 100% lipid-mixing occurred.
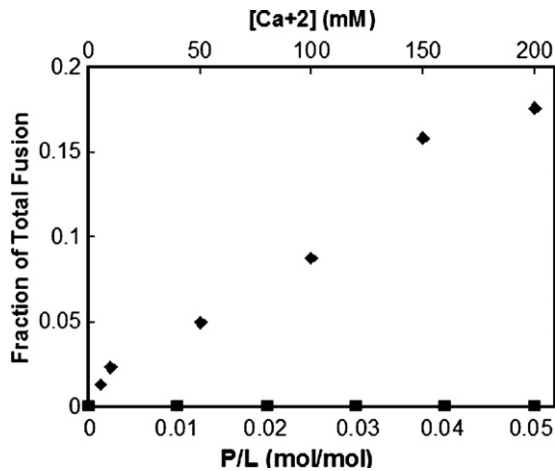
Fig. 5. Contents-mixing assay. 50 μM solutions of POPG LUVs (~100 nm diameter) loaded with either ANTS or DPX were exposed to Crp4 (squares). Quenching of the ANTS fluorescence by DPX reflects the occurrence of contents-mixing. No contents-mixing occurred. Addition of Ca^{+2} to 50 μM solutions of the same type of vesicles caused substantial contents-mixing after only 15 min of incubation (diamonds).

resulting spectrum (as obtained using vesicle solution #3 described in Materials and methods). This assay clearly indicates that Crp4 induces only hemi-fusion (i.e., there is no inner monolayer lipid mixing) at peptide to lipid ratios between 0 and 0.05.

To further confirm the occurrence of hemi-fusion, a contents-mixing assay with POPG vesicles is employed to monitor any mixing of internal vesicle components as a result of vesicle exposure to Crp4. Contents-mixing is manifested by a decrease in fluorescence intensity if vesicles encapsulating fluorescent cargo (e.g., ANTS) merge contents with those containing quenchers (e.g., DPX) (see Materials and methods). Fig. 5 shows that no
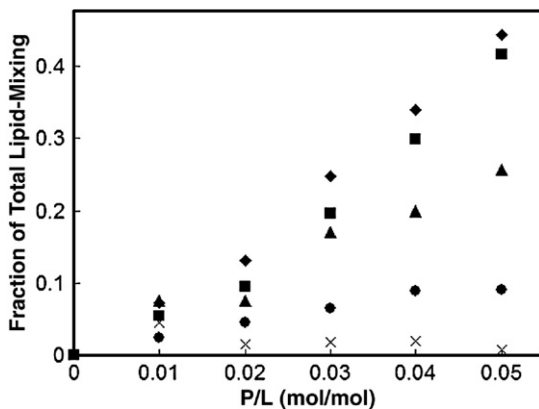
contents-mixing occurs over the same P/L range where substantial outer monolayer lipid-mixing occurs, corroborating the presence of vesicle hemi-fusion within our system. We note that Ca^{+2}, at millimolar concentrations, exhibits the ability to induce complete fusion of POPG vesicles and data for this process is also shown in Fig. 5 to validate the null response obtained when peptide is added to these same vesicles. Our previous research with Crp4 has shown that this peptide can induce leakage of vesicle contents into the extravesicular space to a degree that depends linearly on peptide concentration, with only ~50% contents released at P/L of 0.04 [33]. The leaked probes remain fluorescent because they are diluted into the extravesicular solution; however if enough probe remains in the vesicles quenching would still be observed in the event of contents-mixing. Through independent control experiments we have established that this assay is reliable if leakage is <75%, as it is in our case. All told, the agreement of contents-mixing assays and inner monolayer lipid-mixing assays (which are not affected by leakage) gives full confidence in the finding of peptide-induced hemi-fusion.

2.4. Effect of membrane composition

Lipid-mixing assays were conducted across a range of vesicle membrane compositions as created by mixing the anionic POPG with the zwitterionic POPC. Fig. 6 displays the dependence of lipid-mixing on P/L at various POPG to POPC ratios. The results show an increase in the degree of lipid-mixing with increasing fraction of anionic lipid content. Irrespective of membrane composition, each system exhibits a direct dependence of lipid-mixing on the peptide to lipid ratio, P/L.

2.5. Effect of vesicle curvature

POPG vesicles of various radii were created and used in lipid-mixing assays. As measured by DLS, the vesicles studied

Fig. 6. Membrane composition dependence of lipid-mixing. LUVs (~100 nm diameter) were created of various ratios of anionic POPG and zwitterionic POPC and mixed with Crp4. The non-linear scaling of lipid-mixing with membrane composition (at constant P/L) is most likely a result of the non-linear scaling of membrane charge with membrane composition. Symbols: 98.4 POPG/0.8 NBD-DOPE/0.8 RH-DOPE (diamonds), 73.8 POPG/24.6 POPC/0.8 NBD-DOPE/0.8 RH-DOPE (squares), 49.2 POPG/49.2 POPC/0.8 NBD-DOPE/0.8 RH-DOPE (triangles), 24.6 POPG/73.8 POPC/0.8 NBD-DOPE/0.8 RH-DOPE (circles), 98.4 POPC/0.8 NBD-DOPE/0.8 RH-DOPE (X's).
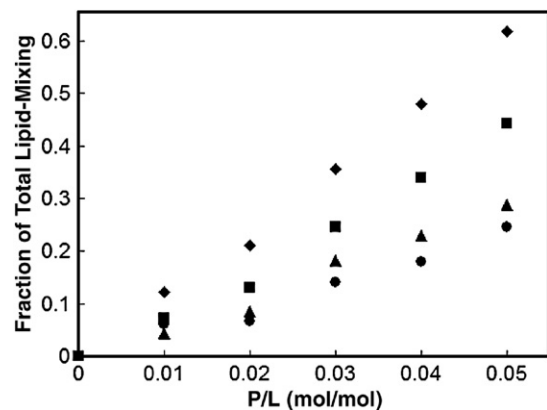

Fig. 7. Vesicle radius dependence of lipid-mixing. POPG and POPG/NBD-DOPE/RH-DOPE vesicles of various radii were created and subjected to Crp4. As radius decreases, the vesicle membrane is more prone to contain defects, thereby yielding more lipid-mixing upon introducing Crp4. Symbols: 15 nm SUVs (diamonds), 47 nm LUVs (squares), 150 nm LUVs (triangles), 1872 nm GUVs (circles).

had radii of 15 nm (SUVs), 47 nm and 150 nm (LUVs), and 1872 nm (GUVs). The degree of lipid-mixing is inversely dependent on the size of the vesicle membrane (Fig. 7). The maximum fraction of lipid-mixing ranges from ~0.20 for GUVs to ~0.60 for SUVs. We note that all SUV and LUV suspensions were fairly monodisperse and had polydispersion indices (PDIs) of 0.06 or less, while the GUV populations contained vesicles with a wide range of diameters and had PDIs as high as 0.45. We believe that the larger vesicles within the GUV suspensions did not undergo lipid-mixing, whereas the vesicles of smaller diameter did. This occurrence most likely overestimates the actual amount of lipid-mixing that would occur in a suspension of monodisperse GUVs (~2 μm in radius).

Because SUVs show an increased propensity for lipid-mixing over LUVs, contents-mixing assays were also conducted on populations of SUVs to test for the occurrence of complete fusion. Contents-mixing did not occur (data not shown). We note that SUVs have a natural tendency to reassemble into larger vesicles due to their thermodynamically unfavorable high membrane curvature [34]. If complete fusion of SUVs did occur in our system, we may not have witnessed a change in fluorescence of the sample due to extensive vesicle leakage. However, we maintain that Crp4 only causes their hemi-fusion. In any case, SUVs are not ideal structures for lipid-mixing and contents-mixing assays due to their inherently metastable nature.

2.6. Effect of lipid-anchored PEG

We have created vesicles containing various amounts of PEGylated lipid for the purpose of observing how this polymer affects the aggregation and hemi-fusion process induced by Crp4. Absorbance measurements (Fig. 8) show that as little as 1% PEGylated lipid in POPG LUVs reduces absorbance by nearly 80%, while increasing the percentage of PEGylated lipid to 5% cuts absorbance by almost 95%. These data clearly

Fig. 9. Effect of PEGylated lipid on Crp4-induced lipid-mixing. POPG LUVs (diamonds) and POPG LUVs with 5% PEG2000-DPPE (squares) were created (both ~100 nm diameter) and mixed with Crp4. As PEG2000-DPPE limits the close approach of vesicles, the extent of lipid-mixing is attenuated accordingly.

demonstrate that the inclusion of PEGylated lipid into POPG vesicles diminishes the resulting aggregation upon introduction of Crp4.

Results from lipid-mixing assays show that PEGylated lipid in POPG LUVs also reduces the occurrence of membrane merger as shown in Fig. 9. At 5% PEGylated lipid, the reduction in lipid-mixing is as much as 75% (at $P/L = 0.05$).

3. Discussion

Hemi-fusion of lipid vesicles is a process that involves the mixing of lipids from the membranes of juxtaposed vesicles but not mixing of the intervesicular contents. The data presented show that Crp4 induces this process among anionic vesicles, with P/L, membrane size, and membrane composition acting as controlling variables. Careful inspection of the data presents two questions meriting discussion: (1) What explains the characteristics of the peptide induced aggregation process, specifically the decay of the aggregation rate to zero and the attainment of a stable aggregate size that increases with P/L? and (2) What is special or different about Crp4–membrane interactions that favor hemi-fusion over fusion?

In the simplest scenario, the formation of hemi-fused vesicle aggregates consists of two steps: (1) the close apposition of vesicle membranes and (2) the union of the outer monolayers of those membranes leading to irreversible lipid-mixing. Vesicle apposition (at constant vesicle concentration) is controlled by Brownian motion (which is dependent upon vesicle size) and is influenced by inter-vesicle forces, such as electrostatics and hydration forces. Addition of the cationic peptide Crp4 to a system of anionic POPG vesicles increases the vesicle collision rate by attenuating the long-range electrostatic repulsion existing between the negatively charged entities. In addition, discrete charge–charge interactions at short-range (e.g., between a multivalent, positively charged peptide on one vesicle and negative lipid on an adjacent vesicle) may also affect the frequency of intimate collisions. Furthermore, binding of Crp4 to a vesicle membrane dehydrates the lipid headgroups, an
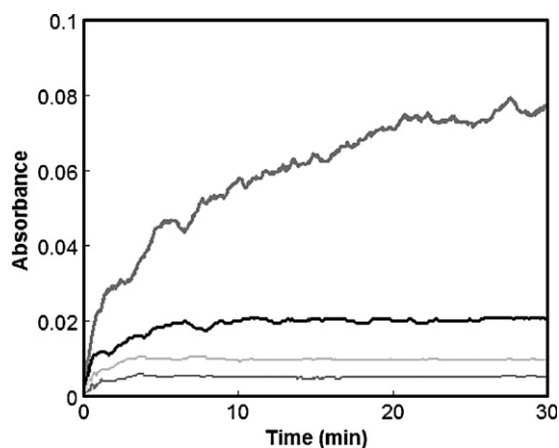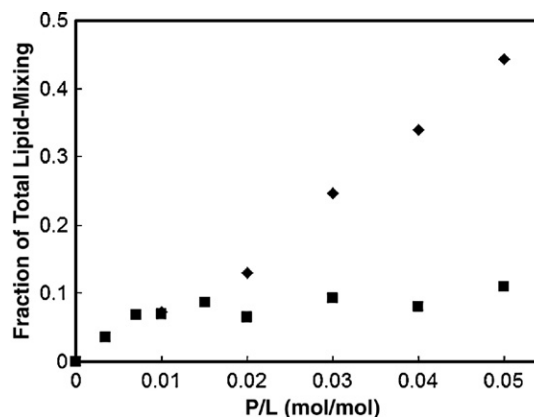

Fig. 8. Effect of PEGylated lipid on Crp4-induced vesicle aggregation. POPG LUVs (thick dark gray line) and POPG LUVs incorporating 1% (thick black line), 2% (thin light gray line), and 5% (thin dark gray line) PEG2000-DPPE were created (all ~100 nm diameter) and exposed to Crp4 at a peptide-to-lipid ratio of 0.05. Increasing amounts of PEG2000-DPPE led to a reduced sample absorbance due to the ability of PEG2000-DPPE to restrict the apposition of vesicles.

action necessary for intermembrane contact [35]. The addition of PEGylated lipid to vesicle membranes acts as a steric barrier restricting the apposition of vesicle membranes and preventing intermembrane contact as revealed in Figs. 8 and 9 [36–38].

It is reasonable to associate an activation energy with the irreversible process of lipid-mixing, the second step in the formation of hemi-fused aggregates, once the membranes are in close apposition. The magnitude of this barrier is dependent on the number of defects existing in the vesicle membrane (with more defects yielding a smaller activation energy), consistent with the work of others who have shown that increases in lipid-mixing result from increased defect density [39,40]. Two distinct mechanisms can generate membrane defects: (1) the inclusion of membrane active agents such as antimicrobial peptides and (2) curvature-induced membrane strain (smaller vesicles are more likely to contain flaws in the membrane due to the strain placed upon packing the lipids into such a tight radius of curvature [12,39,41–44]). We have previously shown the capacity of our peptide, Crp4, to destabilize membranes and induce defects with the use of membrane leakage assays [33,45,46]. The extent of membrane perturbation is directly proportional to the peptide concentration as well as the anionic lipid content in the vesicle membrane. Indeed, the extent of lipid-mixing is also proportional to peptide concentration and fraction of anionic lipid (Figs. 3 and 6). With regard to size-induced defects, we find that lipid-mixing increases as vesicle size decreases (Fig. 7).

Using this two step model of the aggregation/hemi-fusion process, we are able to explain many features of the observed system behavior. The increase of aggregation rate (Fig. 1) and final aggregate size (Fig. 2) with P/L is a reflection of the lower barrier height that results with an increase in the number of membrane defects. Furthermore, the exponential dependence of final aggregate size on P/L manifests the Arrhenius nature of the hemi-fusion process (Fig. 2). The slowing of aggregation at a given P/L leading to a steady-state aggregate size can be associated with a decrease in collision frequency due to slowing of Brownian motion as aggregate size increases; the rate of lipid-mixing may also decrease as aggregate size increases due to subtle changes in membrane curvature related to the hemi-fusion process, as well as depletion of peptide due to translocation (see below).

Within the context of a two step model, we can address the issue of which step is rate controlling. Analysis of our absorbance data (Fig. 1) at time near zero (where the rate is highest), yields an aggregation rate of $2.36e{-}16$ m^3/min at the highest P/L examined (as derived using theory developed by Lichtenbelt et al. to relate turbidity to aggregation rate of non-coalescing particles [47]). This rate can be compared to that predicted by Smoluchowski aggregation theory, where frequency of vesicle collisions (step 1 in the model) determines the aggregation rate. Assuming neutral particles, this predicted aggregation rate is $3.70e{-}16$ m^3/min and only slows to $3.63e{-}16$ m^3/min when accounting for the potentials existing on anionic POPG vesicles [48]. Clearly, this analysis shows that membrane union (step 2) is the rate limiting step in the aggregation/hemi-fusion process.

Lastly, we can offer insight to explain the time scale over which the aggregation rate changes significantly. The decay of

rate is likely associated with a molecular rearrangement process occurring within our peptide–lipid system. Specifically, we have recently discovered that Crp4 translocates across vesicle membranes in a similar time scale over which aggregation transpires (data to be published). Upon injection of vesicles into peptide solution, binding occurs immediately to the outer monolayer, after which the effective P/L decreases with time as peptide distributes itself between both membrane leaflets. Consequently, the defect density within the outer monolayer is initially high and decreases with time, thus controlling the time scale for aggregation.

Turning to the issue of why Crp4 causes hemi-fusion and not complete fusion, we note that our experiments cannot answer this question; however, we can provide insight by comparing what is distinct about the interactions of Crp4 with lipid membranes and those involving peptides that cause complete fusion.

Several common features have been identified among the many peptides that induce complete fusion. Typically, these peptides contain a majority of hydrophobic residues, allowing them to penetrate into the core of lipid membranes, most often inserted in an oblique fashion [10,49–52]. Single amino acid mutations lowering the hydrophobicity of these peptides or altering their orientation of insertion have been found to attenuate or even abolish fusion activity [9,17,53,54]. Crp4, unlike these complete fusion-inducing peptides, is only about 38% hydrophobic and has been shown to reside in a superficially bound state when interacting with lipid vesicles [45,55], possibly lending to its ability to only induce hemi-fusion. As a preliminary experiment, we tested the importance of hydrophobicity for inducing vesicle fusion by creating a hydrophobic mutant of Crp4 where the five glycines in the primary sequence were replaced by leucines. While this mutant did induce more lipid-mixing, we still did not witness any occurrence of contents-mixing (data not shown). These results indicate that hydrophobicity may not be a critical determinant of fusogenic ability, although much more work needs to be conducted to validate this.

The ability to change conformation when binding to lipid membranes is also a common trait among many fusion-inducing peptides [8,56,57]. This change often involves a random coil to α-helix transformation which maximizes favorable interaction of the peptide with the membrane. It is highly unlikely that Crp4 undergoes any change in conformation, as its three disulfide bridges rigidify the β-sheet structure of the peptide. Furthermore, merely the adoption of β-sheet structure may be unconducive for eliciting complete fusion. Experiments with peptides subjected to mutations that disrupt the formation of α-helical structure in favor of a β-sheet structure have shown that these changes were accompanied by a loss of fusogenicity [58–60]. Fujii and coworkers have stated that several human and rabbit defensins, all with β-sheet structure, can induce complete fusion [14]; however, it must be noted that this conclusion was reached only after conducting lipid-mixing assays and not contents-mixing assays, confirming only one of the two requirements for complete fusion. Nieva and coworkers showed that the HIV fusion peptide induces complete vesicle

fusion when assuming a β-sheet structure; however, the presence of Ca^{+2} or Mg^{+2}, two known fusogenic agents, were required [11,61].

Another common feature among fusion-inducing peptides is their tendency to oligomerize. Furthermore, these oligomerized structures are most often trimers or other higher order assemblies [62–64]. Peptides devoid of fusion activity often lack the ability to assemble into oligomers, or only oligomerize to the extent of dimer formation [16,18,65]. NMR studies with Crp4 have shown that this peptide exists as monomers in solution; the membrane bound organization of Crp4 has yet to be determined [66]. Although we have no direct experimental data to determine oligomerization, lipid-mixing data and peptide-induced vesicle leakage data [33,45,46] all scale directly with peptide concentration (and not to a power thereof), consistent with an uncooperative process.

In summary, our survey of the literature shows that most fusogenic peptides possess the following characteristics: largely hydrophobic (>50%), exhibit membrane-induced conformational changes to α-helices, and undergo oligomerization. As Crp4 does not embody these characteristics, it is not surprising that complete fusion is not observed. Exactly why these characteristics promote complete fusion, instead of hemi-fusion, or no fusion, remains an open and interesting question. Equally compelling is the question of what peptide properties are necessary to induce only hemi-fusion, a rarely witnessed occurrence. In the case of Crp4, the peptide is both superficially bound (i.e., limited penetration into the hydrophobic core of the membrane) and is slow to translocate (to be published). This combination leads to a prolonged imbalance in strain across the membrane (from one leaflet to the next), which may impart the elusive conditions for hemi-fusion.

4. Conclusion

We have shown that the β-sheet peptide Crp4 is capable of inducing hemi-fused vesicle aggregates, an uncommon membrane microstructure. We have determined that the rate limiting step in the formation process is the union of juxtaposed vesicle membranes, which is an activated process dependent upon membrane defects as regulated by peptide concentration and vesicle radius. A large degree of control over the aggregation/hemi-fusion process is afforded through manipulation of variables such as membrane charge, membrane composition (e.g., PEGylated lipid), vesicle concentration, and, as mentioned previously, peptide concentration and vesicle size.

Our findings shed new light on the membrane interactions of Crp4 and may even lend insight into the properties of a peptide necessary for inducing hemi-fusion of lipid membranes. The discovery that Crp4 can induce a sustained hemi-fused state of anionic lipid vesicles is one that provokes many ideas for use in practical applications, one of those being the possibility to create multi-compartment vesicular structures for use as drug delivery agents. Presently, hemi-fusion is a rarely witnessed occurrence, but as the membrane interactions of more β-sheet peptides are studied, hemi-fusion may prove to be a more pervasive process.

References

[1] Y. Kozlovsky, L.V. Chernomordik, M.M. Kozlov, Lipid intermediates in membrane fusion: formation, structure, and decay of hemifusion diaphragm, Biophys. J. 83 (2002) 2634–2651.

[2] J.R. Monck, J.M. Fernandez, The fusion pore and mechanisms of biological membrane fusion, Curr. Opin. Cell Biol. 8 (1996) 524–533.

[3] C.P.S. Tilcock, D. Fisher, Interaction of phospholipid membranes with poly(ethylene glycol)s, Biochim. Biophys. Acta 557 (1979) 53–61.

[4] C.P.S. Tilcock, D. Fisher, The interaction of phospholipid membranes with poly(ethylene glycol). Vesicle aggregation and lipid exchange, Biochim. Biophys. Acta 688 (1982) 645–652.

[5] D.E. Leckband, C.A. Helm, J. Israelachvili, Role of calcium in the adhesion and fusion of bilayers, Biochemistry 32 (1993) 1127–1140.

[6] D. Persson, P.E.G. Thoren, P. Lincoln, B. Norden, Vesicle membrane interactions of penetratin analogues, Biochemistry 43 (2004) 11045–11055.

[7] D. Persson, P.E.G. Thoren, B. Norden, Penetratin-induced aggregation and subsequent dissociation of negatively charge phospholipid vesicles, FEBS Lett. 505 (2001) 307–312.

[8] P.A. Bullough, F.M. Hughson, J.J. Skehel, D.C. Wiley, Structure of influenza hemagglutinin at the pH of membrane fusion, Nature 371 (1994) 37–43.

[9] M.J. Gething, R.W. Doms, D. York, J. White, Studies on the mechanism of membrane fusion: site-specific mutagenesis of the hemagglutinin of influenza virus, J. Cell Biol. 102 (1986) 11–23.

[10] C. Harter, P. James, T. Bachi, G. Semenza, J. Brunner, Hydrophobic binding of the ectodomain of influenza hemagglutinin to membranes occurs through the fusion peptide, J. Biol. Chem. 264 (1989) 6459–6464.

[11] J.L. Nieva, S. Nir, A. Muga, F.M. Goni, J. Wilschut, Interaction of the HIV-1 fusion peptide with phospholipid vesicles: different structural requirements for fusion and leakage, Biochemistry 33 (1994) 3201–3209.

[12] J.L. Nieva, S. Nir, J. Wilschut, Destabilization and fusion of zwitterionic large unilamellar lipid vesicles induced by a beta-type structure of the HIV-1 fusion peptide, J. Liposome Res. 8 (1998) 165–182.

[13] H. Qiao, R.T. Armstrong, G.B. Melikyan, F.S. Cohen, J.M. White, A specific point mutant at position 1 of the influenza hemagglutinin fusion peptide displays a hemifusion phenotype, Mol. Biol. Cell 10 (1999) 2759–2769.

[14] G. Fujii, M.E. Selsted, D. Eisenberg, Defensins promote fusion and lysis of negatively charged membranes, Protein Sci. 2 (1993) 1301–1312.

[15] Y. Cajal, J.M. Boggs, M.K. Jain, Salt-triggered intermembrane exchange of phospholipids and hemifusion by myelin basic protein, Biochemistry 36 (1997) 2566–2576.

[16] C. Gray, S.A. Tatulian, S.A. Wharton, L.K. Tamm, Effect of the N-terminal glycine on the secondary structure, orientation, and interaction of the influenza hemagglutinin fusion peptide with lipid bilayers, Biophys. J. 70 (1996) 2275–2286.

[17] M. Horth, B. Lambrecht, M.C.L. Khim, F. Bex, C. Thiriart, J.M. Ruysschaert, A. Burny, R. Brasseur, Theoretical and functional analysis of the SIV fusion peptide, EMBO J. 10 (1991) 2747–2755.

[18] Y. Kliger, A. Aharoni, D. Rapaport, P. Jones, R. Blumenthal, Y. Shai, Fusion peptides derived from the HIV type 1 glycoprotein 41 associate within phospholipid membranes and inhibit cell–cell fusion: structure–function study, J. Biol. Chem. 272 (1997) 13496–13505.

[19] I. Martin, J.M. Ruysschaert, Common properties of fusion peptides from diverse systems, Biosci. Rep. 20 (2000) 483–500.

[20] C.G. Morgan, H. Williamson, S. Fuller, B. Hudson, Melittin induces fusion of unilamellar phospholipid-vesicles, Biochim. Biophys. Acta 732 (1983) 668–674.

[21] I. Cipakova, E. Hostinova, Mammalian antimicrobial peptides, Biologia 58 (2003) 335–341.

[22] A.I. Hobta, P.V. Pogrebnoy, Mammalian peptide antibiotics as regulatory and anticancer agents, Exp. Oncol. 20 (1998) 170–179.

[23] D.M. Hoover, Z.B. Wu, K. Tucker, W.Y. Lu, J. Lubkowski, Antimicrobial characterization of human beta-defensin 3 derivatives, Antimicrob. Agents Chemother. 47 (2003) 2804–2809.

[24] K. Hristova, M.E. Selsted, S.H. White, Interactions of monomeric rabbit neutrophil defensins with bilayers: comparison with dimeric human defensin HNP-2, Biochemistry 35 (1996) 11888–11894.

[25] K. Hristova, M.E. Selsted, S.H. White, Critical role of lipid composition in membrane permeabilization by rabbit neutrophil defensins, J. Biol. Chem. 272 (1997) 24224–24233.

[26] M. Mandal, R. Nagaraj, Antibacterial activities and conformations of synthetic alpha-defensin HNP-1 and analogs with one, two and three disulfide bridges, J. Pept. Res. 59 (2002) 95–104.

[27] P.A. Raj, A.R. Dentino, Current status of defensins and their role in innate and adaptive immunity, FEMS Microbiol. Lett. 206 (2002) 9–18.

[28] A.J. Ouellette, M.M. Hsieh, M.T. Nosek, D.F. Cano-Gauci, K.M. Huttner, R.N. Buick, M.E. Selsted, Mouse paneth cell defensins: primary structures and antibacterial activities of numerous cryptdin isoforms, Infect. Immun. 62 (1994) 5040–5047.

[29] M.I. Angelova, D.S. Dimitrov, Liposome electroformation, Faraday Discuss. 81 (1986) 303–311.

[30] M.I. Angelova, D.S. Dimitrov, Swelling of charged lipids and formation of liposomes on electrode surfaces, Mol. Cryst. Liq. Cryst. 152 (1987) 89–104.

[31] N. Duzgunes (Ed.), Liposomes, Part B, Academic Press, San Diego CA, 2003, pp. 260–274.

[32] P. Meers, S. Ali, R. Erukulla, A.S. Janoff, Novel inner monolayer fusion assays reveal differential monolayer mixing associated with cation-dependent membrane fusion, Biochim. Biophys. Acta 1467 (2000) 227–243.

[33] J.E. Cummings, D.P. Satchell, Y. Shirafuji, A.J. Ouellette, T.K. Vanderlick, Electrostatically controlled interactions of mouse paneth cell alpha-defensins with phospholipid membranes, Aust. J. Chem. 56 (2003) 1031–1034.

[34] K. Edwards, M. Almgren, Solubilization of lecithin vesicles by C12E8: structural transitions and temperature effects, J. Colloid Interface Sci. 147 (1991) 1–21.

[35] T. Stegmann, R.W. Doms, A. Helenius, Protein-mediated membrane fusion, Annu. Rev. Biophys. Biophys. Chem. 18 (1989) 187–211.

[36] G. Basanez, F.M. Goni, A. Alonso, Poly(ethylene glycol)-lipid conjugates inhibit phospholipase C-induced lipid hydrolysis, liposome aggregation and fusion through independent mechanisms, FEBS Lett. 411 (1997) 281–286.

[37] J.W. Holland, C. Hui, P.R. Cullis, T.D. Madden, Poly(ethylene glycol)-lipid conjugates regulate the calcium-induced fusion of liposomes composed of phosphatidylethanolamine and phosphatidylserine, Biochemistry 35 (1996) 2618–2624.

[38] M. Kasbauer, D.D. Lasic, M. Winterhalter, Polymer induced fusion and leakage of small unilamellar phospholipid vesicles: effect of surface grafted polyethylene-glycol in the presence of free PEG, Chem. Phys. Lipids 86 (1997) 153–159.

[39] G. Cevc, H. Richardsen, Lipid vesicles and membrane fusion, Adv. Drug Deliv. Rev. 38 (1999) 207–232.

[40] S.W. Hui, T.P. Stewart, L.T. Boni, P.L. Yeagle, Membrane fusion through point-defects in bilayers, Science 212 (1981) 921–923.

[41] G. Basanez, Membrane fusion: the process and its energy suppliers, Cell. Mol. Life Sci. 59 (2002) 1478–1490.

[42] K. Katsov, M. Muller, M. Schick, Field theoretic study of bilayer membrane fusion. I. Hemifusion mechanism, Biophys. J. 87 (2004) 3277–3290.

[43] V.S. Malinin, B.R. Lentz, Energetics of vesicle fusion intermediates: comparison of calculations with observed effects of osmotic and curvature stresses, Biophys. J. 86 (2004) 2951–2964.

[44] S. Nir, J.L. Nieva, Interactions of peptides with liposomes: pore formation and fusion, Prog. Lipid Res. 39 (2000) 181–206.

[45] D.P. Satchell, T. Sheynis, S. Kolusheva, J. Cummings, T.K. Vanderlick, R. Jelinek, M.E. Selsted, A.J. Ouellette, Quantitative interactions between cryptdin-4 amino terminal variants and membranes, Peptides 24 (2003) 1795–1805.

[46] H. Tanabe, X.Q. Qu, C.S. Weeks, J.E. Cummings, S. Kolusheva, K.B. Walsh, R. Jelinek, T.K. Vanderlick, M.E. Selsted, A.J. Ouellette, Structure–activity determinants in paneth cell alpha-defensins: loss-of-function in mouse cryptdin-4 by charge-reversal at arginine residue positions, J. Biol. Chem. 279 (2004) 11976–11983.

[47] J.W.T. Lichtenbelt, H.J.M.C. Ras, P.H. Wiersema, Turbidity of coagulating lyophobic sols, J. Colloid Interface Sci. 46 (1973) 522–527.

[48] E.R. Wooding, Concentration changes in an aerosol, Proc. Phys. Soc. (1956) 65–70.

[49] P. Durrer, Y. Gaudin, R.W.H. Ruigrok, R. Graf, J. Brunner, Photolabeling identifies a putative fusion domain in the envelope glycoprotein of rabies and vesicular stomatitis viruses, J. Biol. Chem. 270 (1995) 17575–17581.

[50] S.L. Novick, D. Hoekstra, Membrane penetration of sendai virus glycoproteins during the early stages of fusion with liposomes as determined by hydrophobic photoaffinity-labeling, Proc. Natl. Acad. Sci. U. S. A. 85 (1988) 7433–7437.

[51] C.C. Pak, A. Puri, R. Blumenthal, Conformational changes and fusion activity of vesicular stomatitis virus glycoprotein: [^{125}I]iodonaphthyl azide photolabeling studies in biological membranes, Biochemistry 36 (1997) 8890–8896.

[52] G. Schwarz, S.E. Taylor, Thermodynamic analysis of the surface-activity exhibited by a largely hydrophobic peptide, Langmuir 11 (1995) 4341–4346.

[53] D.A. Steinhauer, S.A. Wharton, J.J. Skehel, D.C. Wiley, Studies of the membrane fusion activities of fusion peptide mutants of influenza-virus hemagglutinin, J. Virol. 69 (1995) 6643–6651.

[54] V. Voneche, D. Portelle, R. Kettmann, L. Willems, K. Limbach, E. Paoletti, J.M. Ruysschaert, A. Burny, R. Brasseur, Fusogenic segments of bovine leukemia virus and simian immunodeficiency virus are interchangeable and mediate fusion by means of oblique insertion in the lipid bilayer of their target cells, Proc. Natl. Acad. Sci. U. S. A. 89 (1992) 3810–3814.

[55] D.P. Satchell, T. Sheynis, Y. Shirafuji, S. Kolusheva, A.J. Ouellette, R. Jelinek, Interactions of mouse paneth cell alpha-defensins and alpha-defensin precursors with membranes, J. Biol. Chem. 278 (2003) 13838–13846.

[56] S.D. Fuller, J.A. Berriman, S.J. Butcher, B.E. Gowen, Low pH induces swiveling of the glycoprotein heterodimers in the semliki-forest virus spike complex, Cell 81 (1995) 715–725.

[57] F.A. Rey, F.X. Heinz, C. Mandl, C. Kunz, S.C. Harrison, The envelope glycoprotein from tick-borne encephalitis virus at 2 angstrom resolution, Nature 375 (1995) 291–298.

[58] B.L. Fredericksen, M.A. Whitt, Vesicular stomatitis-virus glycoprotein mutations that affect membrane fusion activity and abolish virus infectivity, J. Virol. 69 (1995) 1435–1443.

[59] B.L. Fredericksen, M.A. Whitt, Mutations at two conserved acidic amino acids in the glycoprotein of vesicular stomatitis virus affect pH-dependent conformational changes and reduce the pH threshold for membrane fusion, Virology 217 (1996) 49–57.

[60] S. Takahashi, Conformation of membrane fusion-active 20-residue peptides with or without lipid bilayers. Implication of alpha-helix formation for membrane fusion, Biochemistry 29 (1990) 6257–6264.

[61] F.B. Pereira, F.M. Goni, J.L. Nieva, Liposome destabilization induced by the HIV-1 fusion peptide effect of a single amino acid substitution, FEBS Lett. 362 (1995) 243–246.

[62] M. Kielian, M.R. Klimjack, S. Ghosh, W.A. Duffus, Mechanisms of mutations inhibiting fusion and infection by semliki forest virus, J. Cell Biol. 134 (1996) 863–872.

[63] T.E. Kreis, H.F. Lodish, Oligomerization is essential for transport of vesicular stomatitis viral glycoprotein to the cell surface, Cell 46 (1986) 929–937.

[64] D.C. Wiley, J.J. Skehel, The structure and function of the hemagglutinin membrane glycoprotein of influenza virus, Annu. Rev. Biochem. 56 (1987) 365–394.

[65] R.A. Parente, L. Nadasdi, N.K. Subbarao, F.C. Szoka, Association of a pH-sensitive peptide with membrane vesicles: role of amino acid sequence, Biochemistry 29 (1990) 8713–8719.

[66] W. Jing, H. Hunter, H. Tanabe, A.J. Ouellette, H. Vogel, Solution structure of cryptdin-4, a mouse paneth cell alpha-defensin, Biochemistry 43 (2004) 15759–15766.